

Tensor Analyzing Power and Current Conservation in the $\vec{d} + p \rightarrow {}^3\text{He} + \gamma$ reaction

S. Nagorny^{1,2}, A.E.L. Dieperink²

¹*NIKHEF, P.O. Box 41882, 1009 DB Amsterdam, The Netherlands*

²*KVI, Zernikelaan 25, NL-9747 AA, Groningen, the Netherlands*

The tensor analyzing power in $p + \vec{d}$ radiative capture is investigated in a covariant and gauge invariant approach. The results of the present calculation are compared with those of other theoretical approaches and with experiment. Predictions for A_{yy} at $E_d = (150 - 350)$ MeV are given. At forward and backward angles T_{20} , T_{22} , and A_{yy} are sensitive to the effects of current conservation.

The interplay between effects coming from the nuclear and current structures is discussed.

PACS numbers: 21.45.+v; 21.30.-x; 25.10.+s; 25.30.Fj.

Key words: gauge invariance, conserved current, radiative capture, tensor analyzing power, external and internal radiation, Ward-Takahashi identities.

I. INTRODUCTION

Radiative capture of the tensor polarized deuterons by protons, and in particular the determination of the tensor analyzing power (TAP) A_{yy} (or the T_{20} , and T_{22} components), has been proposed [1,2] as a unique source of information on the tensor component in the NN interaction, which is responsible for the D waves in few-body systems. A number of full Faddeev calculations have been performed during the last several years in which the three-nucleon dynamics in the bound and the continuum states is taken into account exactly (see [2-3], and references there). Since most of these were restricted to intermediate angles (i.e. near 90° in the c.m.s.) and the low energy region, mostly only $E1$ transitions were considered [2], assuming magnetic dipole and electric quadrupole transitions to be small (as is the case for the cross section). The role of high multipole transitions in A_{yy} was examined only recently [4], although a first estimate of $M1$, $E2$ transitions and their importance was mentioned earlier in [5]. In general, these multipoles appeared to be important even near 90° for $E_d > 30 - 40$ MeV, and at forward or backward angles at all energies. These calculations confirmed the strong sensitivity of the TAP to the D states, and also showed that there are important effects from initial state interactions (ISI) in the three-nucleon continuum.

The reaction mechanism of the radiative capture may be divided into two main classes: “external” and “internal” radiation, corresponding to the emission of the photons from external and internal lines (or vertices), respectively. As was mentioned, the ISI and, therefore, internal radiation in general (of which the ISI is an essential part), is very important in TAP calculations [2-4]. Therefore we expect that meson exchange currents (MEC), reflecting another part of the internal radiation, also play an important role (as they do in the cross section). Moreover, both types of radiation are not independent, they are connected by the requirement of gauge invariance [6,7]. And only an exactly conserved nuclear current guarantees a consistent treatment of the one- and many-body mechanisms [6] with a correct balance of the internal and external radiation [7]. In this connection we note that previous calculations of TAP did not satisfy current conservation, although some effects from MEC were partially included in [2-5] according to Siegert’s hypothesis. An additional iso-vector MEC, which is gauge invariant itself, was included in [5] explicitly for $M1$ - transition.

In this paper we calculate TAP for the $\vec{d} + p \rightarrow {}^3\text{He} + \gamma$ reaction with tensor polarized deuterons, using the covariant and gauge invariant approach [6] developed earlier for photo(electro)- disintegration of the few-body systems [7]. Such an approach based on the effective field theory methods allows one to satisfy the fundamental requirements of covariance CPT- and gauge invariance on both “tree” and “loop” levels, and at the same time to include intra-nuclear dynamics, final (initial) state interaction and effects from MEC. It means, that one- and many-body reaction mechanisms, corresponding to one-particle reducible (pole type) and irreducible (contact type) diagrams, are taken into account consistently with nuclear dynamics and their balance in the total gauge invariant amplitude is guaranteed by the exact conservation of the total nuclear electromagnetic (EM) current. This approach was successfully applied to various observables in the EM interactions of the few-body systems [7-11]. The unpolarized cross sections in the $d + p \leftrightarrow {}^3\text{He} + \gamma$ reaction as well as the cross section and structure functions in the ${}^3\text{He}(e, e'd)p$ channel, which are the most sensitive to final state interaction (FSI) [9], were described well [7,10]. Although, non-relativistic Faddeev calculations also describe the cross section well, some deviations in the description of the structure functions at high transferred momenta, were found [10]. Therefore one expects that spin-observables are even more sensitive to the effects of Lorentz-covariance and current conservation, since they involve the interference of different current components (see, for instance, [12]). That is why it is of interest to study the results for TAP in the framework of the covariant and gauge invariant theory, including all multipole transitions.

In comparing with various approaches, it is convenient to distinguish:

1. Quantum-mechanical approaches, in particular full Faddeev calculations, take into account nuclear structure and ISI (or FSI) exactly, through the solution of the non-relativistic Faddeev equation for bound and continuum state wave functions, preserving orthogonality of the initial/final states. However, there are two main problems: i) gauge invariance is violated, since the mesonic exchange effects, which are implicitly included in the NN- interactions, are not included in the EM interactions, and therefore, there is no balance between one- and many-body EM current operators in the total amplitude (in the restricted low-energy region and for not too extreme angles, a special choice of the EM operators allows one to shift a gauge arbitrariness to high-multipoles, assuming they are not important; but this procedure does not reflect a real gauge freedom, since the gauge is fixed for the main multipoles by some “good choice” of the gauge function, and that is evidently not enough since physical results should not depend upon the choice of the EM operators at all); ii) the non-relativistic structure of EM operators, which are defined in the nucleon rest-frame, requires some corrections in the rest-frame of the nucleus (${}^3\text{He}$), in which frame the Faddeev equation is solved and the calculation of the observables is performed (an additional Lorentz boost of the operators leads to a well-known problem: in the *instant form* of dynamics the corresponding Poincare generators contain the interaction).

2. The field theoretical approach allows one to combine the requirements of covariance and gauge invariance with the accounting for the intra-nuclear dynamics, i.e. ISI/FSI and MEC effects, even for phenomenological NN interactions [6]. However, the complicated structure of the relativistic equations for the n-point Green function (especially in the case of 3- and 4-body systems) and a large number of various “loop” (and vertex) corrections, connected with the inclusion of the regular part of the hadronic T - matrix (in the case of full ISI/FSI), makes it practically impossible for applications at present. That is why we use a compromise [7] which, on the one hand, preserves all above mentioned fundamental properties of the theory, and, on the other hand, allows one to use all achievements of the traditional nuclear physics, such as solutions of the Faddeev equation, and to define various 3- and 4-point nuclear vertex functions. Of course, in this way we lose some relativistic effects (like the small “negative-energy” form factors in nuclear vertices, which are unknown in any case, and very often do not contribute to the main transitions due to the gauge constraints [14-15]), but we preserve a covariance and current conservation, providing a correct balance of the different reaction mechanisms in the total gauge invariant amplitude and, as a result, a correct connection between the (unobservable) wave function and physical amplitudes.

Details of the field theoretical approach to EM interactions of compound systems, including different “minimal” methods leading to the same results for the contact currents on the tree and loop levels, may be found in [6]. All details concerning the $\gamma+{}^3\text{He}\leftrightarrow pd$ reaction, in particular, are given in [7]. In this work we only briefly indicate how to derive the gauge invariant EM amplitudes from the 3- and 4-points Green functions (tdp -, dpn - and $tppn$ - vertices) using “minimal photon insertions” into the external/internal hadronics lines and strong form factors.

II. COVARIANT STRUCTURE OF THE GAUGE INVARIANT AMPLITUDES

First we introduce the general form of the covariant ${}^3\text{He} \rightarrow pd$ vertex ($t = p + d$):

$$A_\nu(p, d, t) = A_\nu^0 + (\not{p} - m_p)A_\nu^{-\cdot p} + A_\nu^{-\cdot t}(\not{t} - m_t) + (\not{p} - m_p)A_\nu^{-\cdot pt}(\not{t} - m_t).$$

Only the first term has a quantum mechanical analogue and can be expressed (in the laboratory system) through the overlap integral of the ${}^3\text{He}$ and ${}^2\text{H}$ wave functions. The next three terms represent so-called “negative-energy” components which do not have a non-relativistic analogue. The last term does not contribute at the tree level, which consists of the pole graphs with only one off-shell particle. We discard all possible, but unknown, negative-energy form components from the beginning. Moreover, the contributions from $A_\alpha^{-\cdot p}$ and $A_\alpha^{-\cdot t}$ terms in any case will be cancelled in the main Dirac (charge) part of the total conserved current in a model independent way (by the corresponding counter terms coming from the contact current) due to the gauge constraint for the 4-point Green function (see [14,15] for details).

The general Lorentz structure of the $A_\alpha^0(p, d, t)$ operator, consistent with the CPT- invariance, is (see [7,13])

$$A_\nu^0(p, d, t) = \{\gamma_\nu D + p_\nu B + d_\nu C\}\gamma_5 \quad (1)$$

However, to eliminate unphysical contributions from the longitudinal components of the wave function of a (virtual) spin-1 particle in a covariant way, we have to satisfy the additional condition (in the same way as for the dpn vertex [6,16]):

$$d_\nu \bar{u}(p)A_\nu^0(p, d, t)u(t) = 0. \quad (2)$$

Note, in the case of the gauge fields unphysical (longitudinal) components (additional polarization states of the vector field) do not contribute automatically due to coupling to the conserved currents (see an example in [14]).

Applying condition (2) to eq.(1), we present the tdp - vertex in the following form, including two independent invariant form factors, D, B , which are related with the S and D components of the overlap integral of the ${}^3\text{He}$ and ${}^2\text{H}$ wave functions [7]:

$$G(t, p, d) = \bar{u}(p)A_\nu^0(t, p, d; -k^2)u(t)\chi_\nu^*(d)$$

$$A_\nu^0(p, d, t) = \{\gamma_\nu D(-k^2) + p_\nu B(-k^2) + d_\nu[bB(-k^2) + aD(-k^2)]\}\gamma_5. \quad (3)$$

Here $u(p)$ is the Dirac bi-spinor, $\chi_\nu(d)$ is the polarization vector (wave function) of a spin-1 particle (deuteron), while t, p, d are the 4-momenta of the ${}^3\text{He}$, proton and deuteron, respectively ($t = p + d$), and k is the relative pd momentum. γ_μ is a Dirac 4×4 - matrix, and $\gamma_5 = i\gamma_0\gamma_1\gamma_2\gamma_3$. All information on the nuclear dynamics is absorbed by the strong covariant form factors $D(-k^2)$ and $B(-k^2)$, which are functions of relative momentum k^2 (see below). The coefficients a and b are given by $a = (\sqrt{t^2} + \sqrt{p^2})/d^2$ and $2b = 1 - (t^2 - p^2)/d^2$.

Note, in ref. [17] a simplified (without physical background) tdp - vertex, expressed in terms of *two* form factors and the relative momentum k only, which is inconsistent with the eqs.(1)-(2), was used. In accordance with CPT- and Lorentz invariance the correct tpd - vertex contains *three* strong form factors, as in eq.(1), and to reduce their amount an additional physical condition should be applied: it cannot be done in an arbitrary way.

In the second step we need to distinguish *reducible* (A_ν^0) and *irreducible* (A_ν^{irr}) vertices (see [6,15], for instance):

$$D_{\mu\nu}^{(0)}(d) S_0(p) A_\nu^0(p, d, t) S_0(t) = D_{\nu\mu}(d) S(p) A_\nu^{irr}(p, d, t) S(t), \quad (4)$$

where $D_{\mu\nu}^0(d)$ and $S^0(p)$ are free Feynman propagators of the vector and spinor particles, while $D_{\mu\nu}(d)$ and $S(p)$ are dressed propagators including the mass-operator (or self-energy part). The 3-point reducible/irreducible vertices (on the left/right hand sides of (4)) satisfy different equations, containing different intermediate states: either free Feynman or fully renormalized propagators. Therefore, it is essential that the selected (from the beginning) type of the vertices (in the left- or right-hand side of (4)) should be used to describe different reaction channels consistently [7,15].

In the next, third, step we derive the 4-point EM Green function from the strong 3-point Green function (tdp vertex). This consists of the “minimal photon insertions” into all external hadronic lines and vertices in eq.(4). It is evident, that such a procedure may be performed using either the left- or right-hand side of eq.(4). In the first (left-hand side) case we obtain a conserved current in terms of reducible vertices and free Feynman propagators, while the second (right-hand side) one generates a conserved current in terms of irreducible vertices and full renormalized propagators. Clearly the physical amplitudes will be equal only if the corresponding currents are conserved [6,15].

To get the simplest structure of the total current we derive a conserved current starting from the left-hand side of the identity (4). This means that we obtain a conserved current in terms of *reducible* vertices and *free Feynman* propagators, while all self-energy parts of the 2-point Green functions are already included into the definition of the vertices. Further we omit the *symbols* 0 at the free propagators and reducible vertices.

Following [7], we get a total conserved current on the tree level which consists of the *external* and *internal* radiation parts:

$$J_{\mu\nu}^{tot}(p, d, q) = J_{\mu\nu}^{extern}(p, d, q) + J_{\mu\nu}^{intern}(p, d, q). \quad (5)$$

The external radiation (fig.1(i)-(iii)) includes the proton, deuteron, and ${}^3\text{He}$ poles (irregular part of the amplitude, generated by the photon insertions into all external lines):

$$J_{\mu\nu}^{extern} = F_\mu(p, p')S_0(p')A_\nu(p', d, t) + A_\lambda(p, d', t)D_{\lambda\beta}^{(0)}(d')F_{\mu\beta\nu}(d', d) + A_\nu(p, d, t')S_0(t')F_\mu(t', t) \quad (6)$$

The internal radiation mechanism (fig.1(iv)) corresponds to a contact current (the regular part, which does not possess pole-type singularities). It is generated by the photon insertion directly into the strong tdp vertex and phenomenologically accounts for the photon radiation from the (virtual) “mesonic sector” (in the mesonic theory of the strong interaction):

$$J_{\mu\nu}^{intern} = \int_0^1 \frac{d\lambda}{\lambda} \frac{d}{dq_\mu} \{z_p A_\nu(p - \lambda q, d, t' - \lambda q) + z_d A_\nu(p, d - \lambda q, t' - \lambda q)\} \quad (7)$$

Here $p' = p - q$, $d' = d - q$, $t' = t + q$, and $z_{p(d)}$ is the charge of the proton (deuteron). The relative variables $k_{p(d)}$ and k (arguments of the strong form factors D, B) in the channels with proton (deuteron) and ${}^3\text{He}$ poles are defined as follows (see [7] for details):

$$k = \eta_d p - \eta_p d, \quad k_p = k - \eta_d q, \quad k_d = k + \eta_p q$$

$$k_{p\lambda} = k - \lambda\eta_d q \quad ; \quad k_{d\lambda} = k + \lambda\eta_p q$$

$$\eta_p = (pt')/t^2 \sim \mu/m_d \quad ; \quad \eta_d = (dt')/t^2 \sim \mu/m_p \quad ; \quad \mu = m_p m_d / (m_p + m_d)$$

It is important that using these equations the integration in (7) may be performed *independent* of the explicit form of the strong form factors $D(-k^2)$ and $B(-k^2)$. (see, for instance, [6,7] and [14,15]). Omitting all terms proportional to q_μ and d_ν (these will not contribute after the contraction with the polarization vector of the photon and/or deuteron: $q_\mu \epsilon_\mu(q) = 0$, $d_\nu \chi_\nu(d) = 0$), we convert the “integral” form (7) of the internal radiation amplitude into the identical “differential” form ($R_\nu(k) = \{\gamma_\nu D(k) + p_\nu B(k)\}\gamma_5$):

$$J_{\mu\nu}^{intern} = \frac{k_\mu}{kq} [z_p R_\nu(k_p) + z_d R_\nu(k_d) - (z_p + z_d) R_\nu(k)] - g_{\mu\nu} [aD(k_p) + B(k_p) + bB(k_d)]\gamma_5 \quad (8)$$

It was shown a long ago (see, for instance, [6,7] and/or [14,15]) that the transition from the “integral” form (7) of the contact current to the “differential” one (8) cannot depend upon the explicit form of the strong interaction due to Lorentz invariance. Expanding the functions $R_\nu(k_{p,d})$ near the k^2 - point at $kq \rightarrow 0$, one can check an important property of the internal radiation amplitude: it has no pole-type singularities [7].

The 3-point EM vertices satisfying the Ward-Takahashi identities (WTI) are (see [6,12,14]):

$$F_\mu(p, p') = F_1(q^2)\gamma_\mu + \frac{F_1(0) - F_1(q^2)}{q^2} \not{q} q_\mu - \frac{\sigma_{\mu\nu} q_\nu}{2m} F_2(q^2), \quad (9)$$

for the interaction with a spinor field, and

$$F_{\mu\alpha\beta}(d, d') = -(d + d')_\mu [g_1 g_{\alpha\beta} - \frac{g_3}{2m_d^2} (q_\alpha q_\beta - \frac{q^2}{2} g_{\alpha\beta})] + (z_d - g_1) \frac{d'^2 - d^2}{q^2} q_\mu g_{\alpha\beta} \\ - 2g_2 (g_{\mu\alpha} q_\beta - g_{\mu\beta} q_\alpha) + g_3 \frac{d'^2 - d^2}{4m_d^2} (g_{\mu\alpha} q_\beta + g_{\mu\beta} q_\alpha - g_{\alpha\beta} q_\mu), \quad (10)$$

for the interaction with a vector field. The EM form factors are normalized by the conditions:

$$F_1^{p(t)}(0) = z_{p(t)} \quad ; \quad F_2^{p(t)}(0) = \kappa_{p(t)} - z_{p(t)} \quad ; \quad g_1(0) = z_d \quad ; \quad g_2(0) = \kappa_d \quad ; \quad g_3(0) = 2g_2(0) - g_1(0) + Q_d,$$

where $z_{p(t)}$ and $\kappa_{p(t)}$ are the charge and magnetic moment of the proton (^3He), while κ_d and Q_d are the magnetic and quadrupole moments of the deuteron.

It is easy to check that the vertices (9), (10) satisfy the WTI also in the half-off-shell case (corresponding wave functions are implied here)

$$(l - l')_\mu F_\mu^{p(t)}(l, l') / z_{p(t)} = S^{-1}(l) - S^{-1}(l') \quad ; \quad (l - l')_\mu F_{\mu\alpha\beta}(l, l') / z_d = D_{\alpha\beta}^{-1}(l) - D_{\alpha\beta}^{-1}(l') \quad (11)$$

Note, that the WTI for the on-shell and half-on-shell γdd - vertices are identical (the same as for the spinor-particles [15]) when the unphysical components of the (virtual) spin-1 particle (deuteron propagator) are eliminated (by the subsidiary condition (2)). Indeed, any terms at the right hand side of the “operator form” WTI (second eq.(11)) proportional to the (virtual) deuteron momenta do not contribute, being contracted with the (only) physical states of the (virtual) deuteron wave function (exactly in the same way as for the real deuteron). Analogously, for the (half-off-shell) γdd - vertex: any terms proportional to the (virtual) deuteron momenta do not contribute to the physical amplitude being coupled to the *physical* states of the (virtual) deuteron wave function (deuteron propagator), exactly in the same way as for the real deuteron.

Using eqs.(11), one can see that the total current $J_{\mu\nu}^{tot}(p, d, q)$ from (5) is exactly conserved for any vertex function ($z_t = z_p + z_d$):

$$\bar{u}(p) q_\mu (J_{\mu\nu}^{extern} + J_{\mu\nu}^{intern}) u(t) \chi_\nu^*(d) = (z_t - z_p - z_d) \bar{u}(p) A_\nu(t', p, d) u(t) \chi_\nu^*(d) = 0. \quad (12)$$

The current (5)-(7) is the minimal necessary set of the reaction mechanisms which obeys current conservation. The three terms in (6) represent the pole-type diagrams, while (7) is the regular part of the amplitude (or contact current). Only the first diagram in fig.1(i) (with a proton pole) corresponds to the plane-wave impulse approximation (PWIA). The second diagram in fig.1(ii) (with a deuteron pole) corresponds to the crossing-channel (recoil mechanism), while

the third diagram in fig.1(iii) with the ${}^3\text{He}$ pole is part of the ISI/FSI [7,12] (it is the dominant one, at least near threshold), caused by the pole-part of the hadronic T - matrix of the elastic $pd \rightarrow pd$ scattering in the initial (or final) state [6]. As it may be seen from the explicit form of the contact current (8), its value is determined by the deviation of the nuclear wave functions (and overlap integrals) from their long-range asymptotics [6,14]. A contact part of the amplitude (see fig.1(iv)) corresponds to a many-body current and effectively (implicitly) accounts for the effects associated with MEC (in the framework of the meson theory of NN- interaction) [6].

Although the contact current does not contain pole-type singularities, it must be included on the “tree”-level, since it is the contact diagram that provides conservation of the nuclear current for the class of pole graphs. Note, that the requirement of a “minimal trajectory” (the path of integration in (7)) fixes the contact amplitude in a unique way [6,14,15]. Let us specify what we mean, since sometimes in the literature the “arbitrariness” of the procedure/prescription to reconstruct gauge invariance has been discussed. As it is well known, the requirement of gauge invariance itself does not allow one to reconstruct a “transverse” (gauge invariant by itself) part of the contact current. But it does not mean that an arbitrary gauge invariant construction can be added to the current (7): any contributions to the physical amplitude must be based on the concrete physical mechanisms only. In a phenomenological approach (when we do not specify the mechanisms of the strong NN- interaction) an additional (fundamental) condition should be used together with the gauge constraint to fix the contact current in a unique way. In a “minimal” field-theoretical scheme [6,14] an additional requirement of the “minimal trajectory” is implied so that the “transverse” part may only be equal to zero. Indeed, any non-zero “transverse” contribution may be directly converted into a deviation from the “minimal trajectory” and violation of the “minimal scheme”. In this way a purely “transverse” part of the amplitude (which is equal to zero on the tree-level) should be considered as a correction and must be calculated through the next-order class diagrams (one-loop corrections) using the same “minimal scheme” on the level of two-body irreducible graphs (see ref. [6]). Such a “step-by-step” approach allows for a consistent gauge invariant description of the effects associated with FSI and MEC, selecting diagrams in accordance with one-, two-, ..., n - particle reducible/irreducible contributions and applying the “minimal scheme” on each level separately. This is a convenient approach in case when we do not know the lagrangian, but we do know all hadronic Green functions (n -point vertices). For example: 1) if we know only 3-point nuclear vertex (tpd - vertex in our case) we can generate only tree-level gauge invariant amplitude; 2) if we know 3- and 4-point nuclear vertices (i.e. tpd -, $tpnn$ - and $pdpd$ - vertices) we can generate not only a gauge invariant tree-level amplitude, but also a new gauge invariant set of one-loop contributions (i.e. that purely “transverse part” of the contact current which was equal to zero on the tree-level); 3) if we know the 3-, 4- and 5-point vertices (i.e. tpd -, $tpnn$ -, $pdpd$ - and $pdpnn$ - vertices) we can generate an additional gauge invariant set of two-loops contributions (that is a correction to the pure “transverse part” of the contact current associated with two-body irreducible contributions). This procedure in principle may be continued selecting three-, four-loop corrections and so on (see [6,7]). For our particular reaction a pure transverse part of the contact amplitude is a correction, accounting for the regular part of the pd - scattering T - matrix, and must be generated through the same “minimal photon insertions” into all internal lines and vertices of the loop-diagrams in the equations for the nuclear vertices. However, in the present paper we will neglect such a contribution.

In addition to the tree level diagrams we also include the nearest non-pole contributions (see fig.1(v),(vi)): one-loop corrections to the current (5) whose singularities are the closest to the “physical region” after the pole-type diagrams. Diagrams in fig.1(v),(vi) correspond to the photon production due to the transformation of the deuteron into a spin-singlet pn - pair: $d \leftrightarrow \gamma + \{pn\}_S$ [7]. These cannot be included at the tree level, since there is no bound state in a spin-singlet pn - system. Such a spin-isospin-flip transition represents an *isovector* current, contrary to the *isoscalar* one in eq.(5) (see also [8]). Although it also belongs to the *internal radiation* class, it evidently cannot be taken into account by the diagram in fig.1(iv). The isovector current in fig.1(v),(vi) may be presented in the form [7] ($p_2 = p_1 + q$, $t = p_1 + n + p$, $n + p_2 = d$):

$$J_{\mu\nu}^{\{pn\}_S} = -i \int \frac{d^4n}{(2\pi)^4} \{Tr[S(p_2)F_\mu(p_2, p_1)S(p_1)A_s(p, p_1, n)S^T(n)\bar{\Gamma}_\nu^{dpn}(n, p_2)] + (p \leftrightarrow n)\} \quad (13)$$

The 4-point nuclear vertex $A_s(p, p_1, n)$ of the virtual ${}^3\text{He} \rightarrow p + \{pn\}_S$ break-up with a spin-singlet pn - pair contains a strong form factor G_s which is a combination of the S - and S' - components of the ${}^3\text{He}$ wave function [7,9]:

$$\bar{u}(p)\bar{u}(p_1)\bar{u}(n) A_s(p, p_1, n) u(t) = G_s [\bar{u}(p)u(t)] [\bar{u}(p_1)\gamma_5 C\bar{u}^T(n)], \quad (14)$$

where C is the charge conjugation matrix.

Using (14) and the explicit form of the dpn vertex Γ_ν^{dpn} [16], we get from (13):

$$J_{\mu\nu}^{\{pn\}_S}(p, d, q) = -i \int \frac{d^4n}{(2\pi)^4} \frac{G_s}{n^2 - m^2 + i\epsilon} \frac{I_{\mu\nu}}{p_2^2 - m^2 + i\epsilon} \quad (15)$$

$$\begin{aligned}
(4im)^{-1}I_{\mu\nu} &= (\mu_p - \mu_n)\Gamma_1\epsilon(dq\mu\nu) + (\kappa_p - \kappa_n)\left[\left(\frac{dn}{m^2} - 1\right)\epsilon(dq\mu\nu) - 2\epsilon(nq\mu\nu)\right]\Gamma_1 \\
&+ [(\mu_p - \mu_n)\Gamma_2 + (\kappa_p - \kappa_n)(\Gamma_1 - \Gamma_4)]\frac{n_\nu}{m^2}\epsilon(dq\mu n),
\end{aligned} \tag{16}$$

where $\Gamma_{1,2,\dots,4}$ are strong form factors in the dpn vertex (without the “negative-energy” form factors, $\Gamma_3 = 0$). Their expressions in terms of the deuteron wave functions may be found, for instance, in [6,16]); we also introduced $\epsilon(abcd) = \epsilon_{\mu\nu\alpha\beta}a_\mu b_\nu c_\alpha d_\beta$.

Taking into account that $q_\mu I_{\mu\nu} = 0$ independent of the strong dynamics (due to the fact that all fully antisymmetric tensors $\epsilon_{\mu\nu\alpha\beta}$ in (16) contain already the vector q), we see that the current (14) is always conserved:

$$q_\mu J_{\mu\nu}^{\{pn\}S}(p, d, q) = 0.$$

We note that the isovector internal radiation amplitude (13), $J_{\mu\nu}^{\{pn\}S}$, is sometimes approximated in the literature by the introduction of the external radiation diagram with a “scalar deuteron” (d^*) pole (see ref. [17], as an example). However, such a simplification is inconsistent, since it requires additional (free) parameters and/or special assumptions for the tpd^* vertex (replacing the unbound d^* wave function by a bound one, for instance). As was found recently (see [7-9]), the isovector transition (with spin-isospin-flip) is very important for the cross sections [8,10] and spin observables [9]. That is why a consistent treatment of the spin-singlet pairs is essential.

As a last step, to get a numerical result, we need to define all strong form factors appeared in eqs. (3), (15)-(16). Since solutions of the corresponding relativistic equations are not available at the moment, we express all form factors through the corresponding wave functions (and/or overlap integrals) in the laboratory system (i.e. in the system where the solution of the Faddeev equation is obtained), in the same way as it was done for the form factors in the $d \rightarrow pn$ vertex [16]:

$$\left(\frac{p^2}{2\mu} + \epsilon_2\right)^{-1}D(p) \sim I_0(p) + I_2(p)/\sqrt{2}, \quad \left(\frac{p^2}{2\mu} + \epsilon_2\right)^{-1}m_p B(p) \sim I_0(p) + \sqrt{2}\frac{4m^2}{p^2}I_2(p), \tag{17}$$

$$\left(\frac{\vec{l}^2}{2\mu} + \frac{\vec{k}^2}{m} + \epsilon_3\right)^{-1}G_s(l, k) \sim \Psi^S(l, k) + \Psi''(l, k), \tag{18}$$

where $I_{0(2)}(p)$ is the $S(D)$ - part of the overlap integrals between ${}^3\text{He}$ and ${}^2\text{H}$ wave functions, while Ψ^S and Ψ'' are the fully symmetric and mixed symmetry components, respectively; $\epsilon_{2(3)}$ is a binding energy in the two-(three-)body break up channel.

In the case of the isovector transitions (transformation of a spin-singlet pn - pair into a deuteron) the last two diagrams in fig.1(vii),(viii) do not contribute if we neglect “negative-energy” form factors (P - waves) in the dpn vertex. We will also neglect “non-pole” type contributions from the orthogonal states of unbound pn pairs in a spin-triplet states which appeared to be too small in a wide kinematical region [7,8,10], since the main contribution from the spin-triplet pn pair is already taken into account by the deuteron-pole diagram (see fig.1(ii)).

III. NUMERICAL RESULTS AND CONCLUSIONS

For numerical calculations we use the solutions of the Faddeev equations with Reid Soft Core (RSC) [18], and Argonne-V18 + Urbana-IX [19] (V18) interactions. By comparing these we obtain an estimate of the sensitivity of the TAP to various models of the nucleon-nucleon potential. Moreover, since the TAP is mostly determined by the small admixture of D states components (which is at the level of 8%) in the vertex functions (see [1-4]), the comparison of the results for different models of NN interaction with the experiments could provide a separation of the effects coming from the nuclear dynamics and the structure of the EM current.

Fig.2 shows a comparison of the existing calculations for T_{20} with the experimental results at $E_d = 19.6$ MeV. As one sees the present results (including all multipole transitions) for the RSC and V18 interactions are very close; they describe the experimental points well, reproducing the asymmetric behaviour around 90° and even the (same) trend at forward/backward angles.

The results of ref. [2] (symmetric around 90°), based on the full Faddeev calculations for the bound and continuum state wave functions with the Paris potential, contain $E1$ transitions only. These describe the experimental points for T_{20} at intermediate angles only, indicating the need to include, at least, $M1$ and $E2$ multipoles even at such a low

energy. Comparing the present results and those from ref. [2], one can see that at *forward/backward* angles in both cases T_{20} has the same sign: *positive* in our case, and *negative* in the case of ref.[2]. Of course, this is not surprising, since magnetic multipoles (which are not included in ref. [2]) are important at extreme (small/large) angles.

However, a further comparison with the results reported in ref. [4], which are also based on full Faddeev wave functions with the Bonn potential (for the initial/final states), but include all multipole transitions, contrary to the ref. [2], shows a *positive/negative* “asymmetry” of the T_{20} at *forward/backward* angles. However, our present gauge invariant calculations (solid- and dashed-curves in fig.2), which also include all multipoles, do not show the change of the T_{20} - sign with increasing the angle from 0° to 180° . We note that an “asymmetric” behaviour of T_{20} observed in ref.[4] for forward/backward directions cannot be the result of the inclusion of the full ISI. Our present PWIAS (not gauge invariant) calculation, i.e. accounting for the proton + deuteron poles (fig.1i+1ii) in the Coulomb gauge and the iso-vector current (13) (fig.1v+1vi), quantitatively reproduces the same “asymmetric” behaviour of T_{20} with the negative (positive) signs at forward (backward) angles (we do not show this not gauge invariant calculation, since it has no physical meaning). However, inclusion of all other diagrams, which restore current conservation, makes T_{20} again “symmetric”, as it is in fig.2, for any NN - interactions. Taking into account that this effect does not depend on the type of NN interaction (compare our present results for RSC and/or V18 with the ones in ref.[4]), we suggest that the different behaviour of T_{20} at extreme angles is connected with the effects of current conservation which provides a consistent treatment (or a correct balance) of the *external* and *internal* radiations. In other words: the observed effect appears to be connected with the structure of the total current, but not with the nuclear structure, since it exists for various realistic NN models.

From the comparison of the theoretical curves in fig.2 with the experimental results in the intermediate angle region, where TAP was proposed to be used as a test of the tensor forces [1,2], we can conclude that, in general, all realistic potentials (V18, Bonn, Paris and RSC) contain a reasonable D components at small momenta (which are tested by the deuterons with $E_d = 19.6$ MeV). Although, the V18 and Bonn potentials give better agreement with experiment near $\theta = 90^\circ$ (where high multipoles, and an exact balance of the internal/external radiations are not very important at this particular energy), the accuracy of the measurements is clearly not enough to make a choice.

In fig.3-5 the present calculations are compared with the experimental results at $E_d = 29.0; 45.0; 95.0$ MeV, as well as with previous full Faddeev quantum mechanical calculations [4], where the *Siegert hypothesis* was used. All figures clearly indicate an increase of the difference between the covariant and non-relativistic calculations at forward/backward angles with the increasing of the deuteron energy. Moreover, at high energies (see fig.5) the disagreement appears at all angles. Unfortunately, the existing experimental results cover only intermediate angle region. Therefore, we would like to stress the need for new measurements of TAP in wide angle region for any possible energies. This could allow one to check the sensitivity of TAP to relativistic effects and current conservation.

A comparison of the present and previous [4] calculations in the intermediate angle region shows that both results are very close at $70^\circ < \theta < 130^\circ$, contrary to the forward/backward angle region (see fig.3,4). This clearly confirms a well known fact [20] that at low energies ($E_d < 50 - 60$ MeV) and for the angles near 90° it is not so important (for any observable, including TAP) whether external and internal radiations (pole and contact currents) are included consistently. The matter is: in the above mentioned conditions the Siegert hypothesis “works” well enough (the $E1$ - transition dominates) and a “current conservation” may be arranged artificially using the continuity equation to express the longitudinal current components in terms of the charge- density operators. This corresponds to a “good choice” of the EM- operators when the gauge is fixed for the main multipole transitions, while transferring the gauge-arbitrariness to the high multipoles [20]. Since the later are not important at small energies, this makes a non-gauge invariant theory practically independent of the gauge arbitrariness in these very restricted kinematics conditions (certainly, such a procedure does not reflect full *gauge freedom* for all multipoles). Indeed, as one can see from fig.5, this is not the case already at $E_d = 95$ MeV, where the Siegert hypothesis does not work. The same situation appears at forward/backward angles, but in this case at all energies.

Therefore we may conclude: the comparison of both calculations (the present one and those from [4]) with the experimental results at $E_d = 29.0$ and 45.0 MeV for the middle-angle region near $\theta = 90^\circ$ in fig.3,4 shows that in the Bonn and Argonne-V18 potentials the tensor forces are presented reasonably well, in general. However, it seems that at 29.0 MeV the D components are only a bit overestimated (see fig.3) by both potentials, although, evident lack of experimental points even in the middle-angle region does not allow to make more complete conclusions. As for the $E_d = 95$ MeV, even in the intermediate angle region, TAP strongly depends upon both reaction mechanisms and nuclear structure (see fig.5), and it is not possible to make any concrete conclusions about D - states when the *external* and *internal* radiations are not included consistently with nuclear dynamics, in a gauge invariant way. Further measurements of TAP at high energies could provide an excellent test of the total conserved nuclear current, and could be used to get a consistent information about tensor-forces.

In fig.6 we present a set of predictions for TAP at various energies: from $E_d = 150$ MeV up to 350 MeV. Such measurements could be performed, for instance, at KVI, IUCF, TRIUMF, and could be used as a filter of different theoretical approaches and models for NN interactions. To show that the present approach predicts, at least, the

absolute values of the cross sections in the above mentioned energy interval, we compared in fig.7,8 our results (solid curves) for ${}^3\text{He} + \gamma \rightarrow p + d$ reaction with the most complete at the moment (for such energies) non-relativistic calculations [21]. In the diagrammatic approach of J.M. Laget [21] the two- and tree-body MEC (dashed and dashed-dotted curves, respectively) are included in addition to the FSI and PWIA diagrams. From a comparison in fig.7,8 with the experiments at $E_\gamma = 240$ MeV, and 340 MeV (see references in [21]) we conclude that the present calculations (solid curves) describe the existing experimental results on the cross sections in general. Although, estimation of the loop-corrections, associated with the regular part of the $pd \rightarrow pd$ T - matrix, would be interesting from the theoretical point, the experimental uncertainties are still too large and new measurements are needed.

To summarize, in the $\vec{d} - p$ radiative capture the TAP is very sensitive to the effects of current conservation and consistent treatment of the external and internal radiation mechanisms at extreme *forward/backward* angles even at small initial energies. Although, at intermediate angles and at $E_d < 50 - 60$ MeV, TAP indeed may discriminate between various NN interactions in accordance with their tensor forces, the exact conservation of the EM current becomes important in TAP calculations at all angles starting from $E_d > 70 - 80$ MeV.

After completion of this work two calculations of the radiative pd - capture appeared [24,25].

In [24] authors used basically the same approach, as was developed in ref.[7], but with some approximations (see [26] for details). For instance, a simplified tdp -vertex (as in [17]), depending on the relative pd - momentum only, was used (see eq.(11) of ref [24]), and the spin-singlet pn - pairs were approximated by the quasi-bound “scalar deuterons”. Furthermore, the use of a “self-energy” correction to the ${}^3\text{He}$ - propagator in ref.[24] is not consistent with the use of a reducible tdp - vertex which already includes all self-energy parts (see eq.(4)). At last, accounting for the ISI by the modification of the tdp - vertices in the pole-graphs in accordance with eq.(40) from [24] violates T - reversal invariance, since leads to an imaginary part in the vertices defined by the bound states wave functions only. Generating an imaginary part in the tpd - vertex and violating T - invariance, the authors of [24] tried to account for the *many-body* ISI effects through the *one-body* (pole-type) currents, that is not possible in principle.

In [25] J.Golak et al. have shown that an (explicit) inclusion of MEC considerably changed their previous calculations on T_{20} , especially at 19.8 MeV. Their new result is shown in fig.2 by the double-dashed curve. As it may be seen, inclusion of MEC changes the character of their former result (dashed-dotted curve) at small angles and comes on closer to our calculations (solid and dashed curves in fig.2). In general, the trend of their new calculation at $\theta < 50^\circ$ coincides now with our results (compare double-dashed curve with the solid- and dashed- lines), in a full agreement with the discussion in Sec.III (see above). As for the higher energies, the new calculations [25] differ only slightly from the previous ones [4], reproducing the same shape of the curves, and we do not show them. In addition, authors of [25] have found that after inclusion of MEC their calculations become less sensitive to the model of NN- interaction. That is exactly what we described in Sec.III: when one- and many-body currents are (correctly) balanced in the total amplitude, various realistic potentials lead to close results.

IV. ACKNOWLEDGEMENTS

This work is supported in part by the Stichting Fundamenteel Onderzoek der Materie (FOM) with financial support of the Nederlandse Organisatie voor Wetenschappelijk Onderzoek(NWO). We are grateful to W. Gloeckle, J. Golak, H. Vitala, A. Fonseca, I. Sick, V. Pandharipande and N. Kalantar for the stimulating discussions and for providing numerical theoretical and/or experimental results. In particular we would like to thank R. Wiringa, who provided us with his calculations of the ${}^3\text{He}$ wave functions and various overlap integrals for the Argonne-V18 potential.

-
- [1] A. Arriaga and F.D. Santos, Phys.Rev., **C29** (1984) 1945.
 - [2] A.C. Fonseca and D.R. Lehman, Phys.Lett., **B267** (1991) 159; Phys.Rev., **C48** (1993) R503; priv. comm., 1998.
 - [3] S. Ishikawa and T. Sasakawa, Phys.Rev., **C45** (1992) R1428.
 - [4] H. Anklin, L.J. de Bever, S. Buttazzoni et al., Nucl. Phys., **A636** (1998) 189; priv. comm. 1999.
 - [5] J. Jourdan, M. Baumgartner, S.Burzynski et al., Nucl. Phys., **A453** (1986) 220.
 - [6] S.I. Nagorny et al., Sov.J.Nucl.Phys., **49** (1989) 465; **53** (1991) 228.
 - [7] S.I. Nagorny et al., Sov.J.Nucl.Phys., **55** (1992) 1325; Phys.of Atom.Nucl., **57** (1994) 940.
 - [8] C.Tripp, G. Adams, P. Stoler et al., Phys.Rev.Lett., **76** (1996) 885.
 - [9] S.I. Nagorny and W. Turchinets, Phys. Lett., **B389** (1996) 429; **B429** (1998) 222.
 - [10] C. Spaltro, H. Blok, E. Jans et al., Phys. Rev.Lett., **81** (1998) 2870.

- [11] J.v. Leeuwe, H. Blok, E. Jans et al., Phys. Rev.Lett., **80** (1998) 2543.
- [12] S.I. Nagorny et al., Phys.Lett., **316** (1993) 231.
- [13] J. Govaerts et al., Nucl.Phys., **A368** (1981) 409.
- [14] S.I. Nagorny, Proc. BLAST Workshop, 1998, <http://mitbates.mit.edu/~blast/workshop>.
- [15] S.I. Nagorny and A.E.L. Dieperink, Eur. Phys. J. A5 (1999) 417.
- [16] R. Blankenbecler and L.F. Cook, Phys.Rev., **119** (1960) 1745; W.W. Buck and F. Gross, Phys.Rev., **D20** (1979) 2361.
- [17] G. Faldt and L.-G. Larsson, J.Phys.G: Nucl.Part.Phys., 19(1993)171; 569; 987; 1003.
- [18] C.H. Hajduk, A.M. Green, and M.E. Sainio, Nucl. Phys., **A337** (1980) 13.
- [19] R. Schiavilla, V.R. Pandharipande and R.B. Wiringa, Nucl.Phys., **A449** (1986) 219; J.L. Forest, V.R. Pandharipande, S.C. Pieper, R.B. Wiringa, R. Schiavilla and A. Arriaga, Phys.Rev. **C54**(1996)646; B.S. Padliner et al., Phys.Rev., **C56** (1997) 1720; priv. comm. 1998.
- [20] S.I. Nagorny, Yu.A. Kasatkin and V.A. Zolenko, Proc. of 8th- Int. Seminar on “Electromagnetic Interactions of Nuclei at Low and Medium Energies”, Moscow, 1992, p.43-50.
- [21] J.-M. Laget, Phys.Rev., **C38** (1988) 2993.
- [22] M.C. Vetterli et al., Phys.Rev.Lett., **54** (1985) 1129.
- [23] W.K. Pitts et al., Phys.Rev., **C37** (1988) 1.
- [24] A.Yu. Korchin, D. Van Neck, O. Scholten and M. Waroquier, Phys.Rev., **C59** (1999) 1890.
- [25] J. Golak, H. Kamada, H. Vitala, W. Gloeckle et al., Phys.Rev., **C62** (2000) 054005; priv. comm. 2001.
- [26] S. Nagorny, Phys.Rev., **C** (2001) , (to be published)

Figure captions

Fig.1

Gauge invariant set of covariant diagrams for the two-body ^3He -photodisintegration (or radiative dp - capture).

Fig.2

T_{20} at $E_d = 19.6 \text{ MeV}$. The solid (dashed) curve presents our covariant and gauge invariant calculations (all multipoles) with RSC (Argonne-V18) NN - interaction. The dotted and dashed-dotted curves show the quantum-mechanical calculations from ref. [2] ($E1$ multipole only) with Paris potential and ref. [4] (all multipoles) with Bonn potential, respectively. The double-dashed line presents new calculations from ref. [25] (the same as in ref. [4], but with additional MEC - contributions). The data are from ref. [21].

Fig.3

Tensor analyzing power A_{yy} at 29 MeV . The solid curve corresponds to our present calculations with the Argonne-V18 interaction. The dashed curve reproduces the full result obtained in ref. [4] with the Bonn potential. The experimental point is from ref. [5].

Fig.4

Tensor analyzing power A_{yy} at 45 MeV . The solid curve corresponds to our present calculations with the Argonne-V18 interaction. The dashed curve reproduces the full result obtained in ref. [4] with the Bonn potential. The data are from ref. [4].

Fig.5

Tensor analysing power A_{yy} at 95 MeV . The solid curve corresponds to our present calculations with the Argonne-V18 interaction. The dashed curve reproduces the full result obtained in ref. [4] with the Bonn-B potential. The data are from ref. [22].

Fig.6

Our predictions for the tensor analysing power A_{yy} at various energies. The solid curve corresponds to $E_d = 150 \text{ MeV}$, while dashed, short-dashed, dotted and dashed-dotted represent our results for $E_d = 200, 250, 300 \text{ and } 350 \text{ MeV}$.

Fig.7

The cross section for the $^3\text{He} + \gamma \rightarrow p + d$ reaction at $E_\gamma = 240 \text{ MeV}$. The solid curve corresponds to our present covariant and current conserved calculations with Argonne-V18 interaction. The dashed (dashed-dotted) curve shows J.-M. Laget calculations from ref. [20] in the diagrammatic approach with 2-body (3-body) MEC and FSI. See for the data in ref. [20].

Fig.8

The same as in fig.7, but for $E_\gamma = 340 \text{ MeV}$.

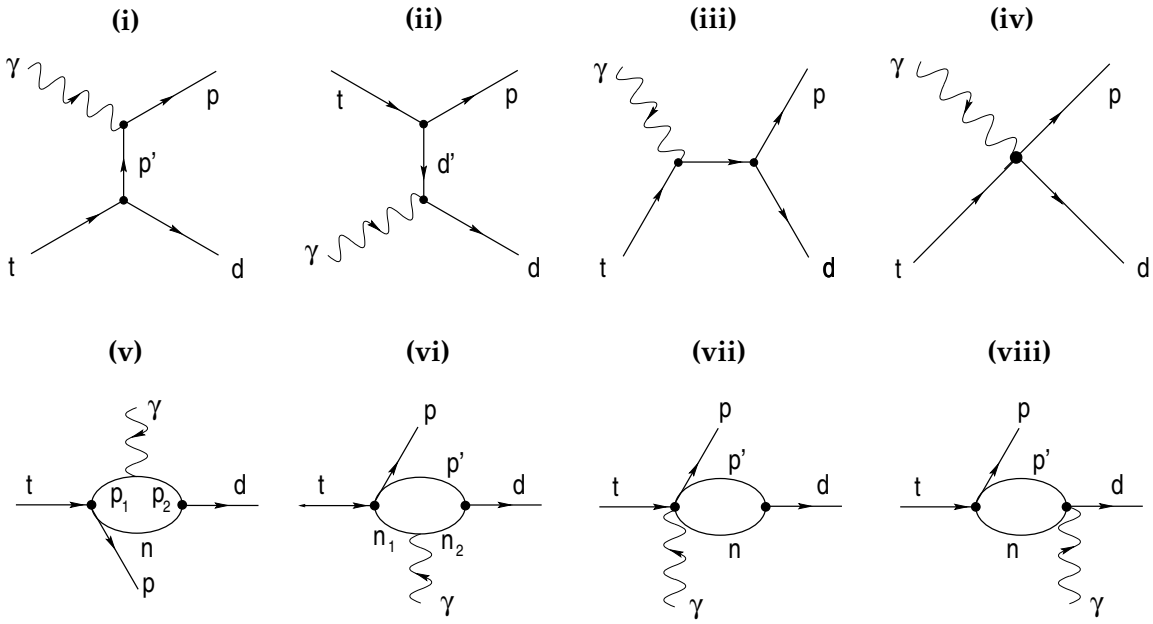


FIG. 1.

FIG. 2.

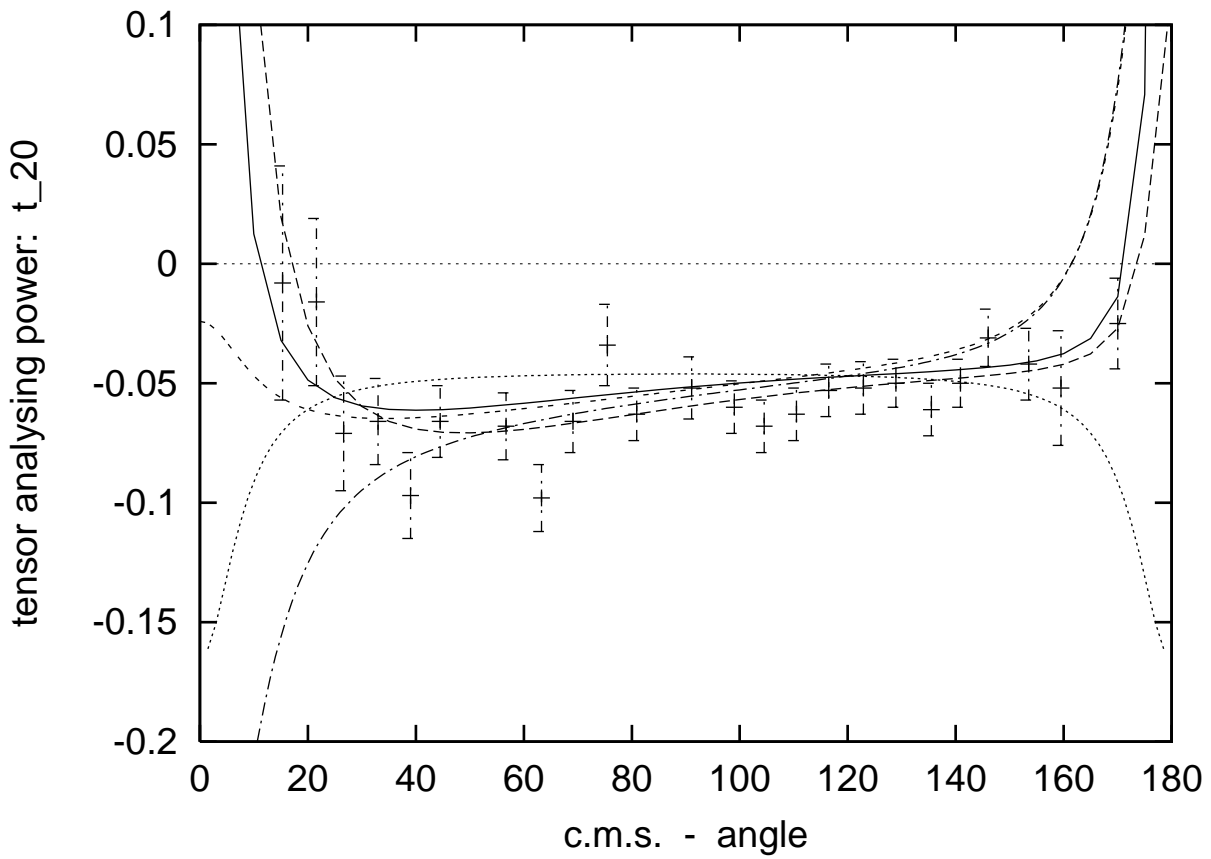


FIG. 3.

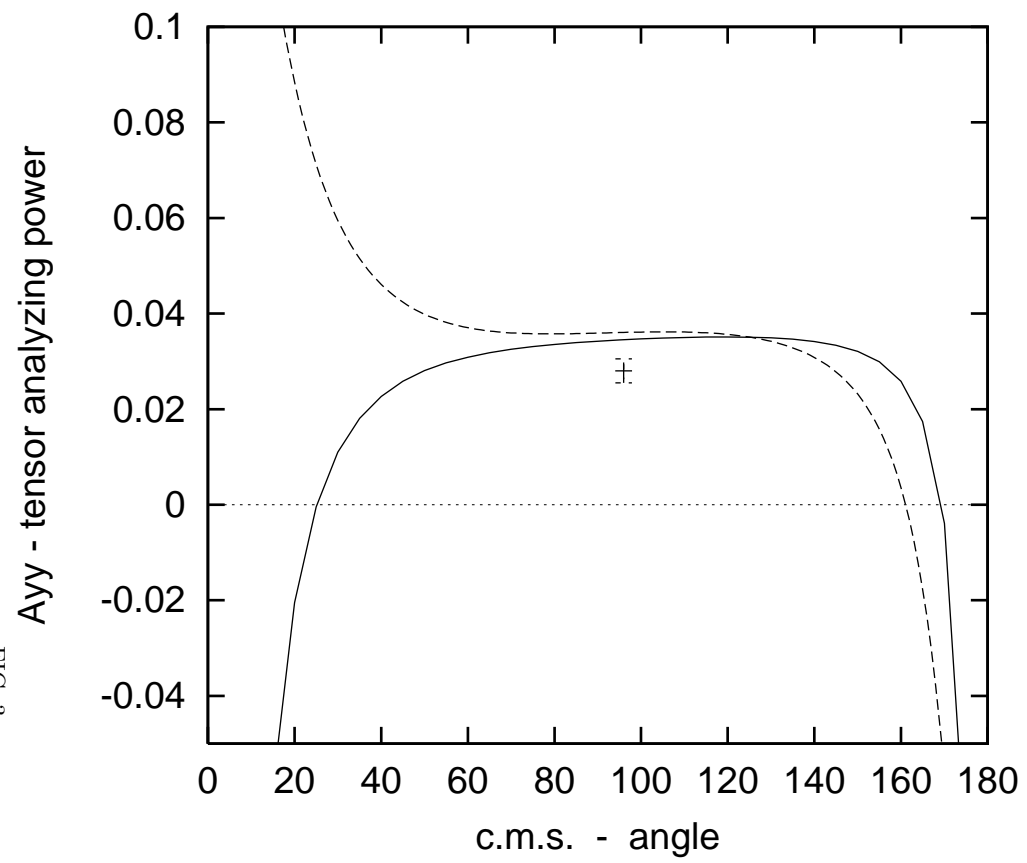


FIG. 4.

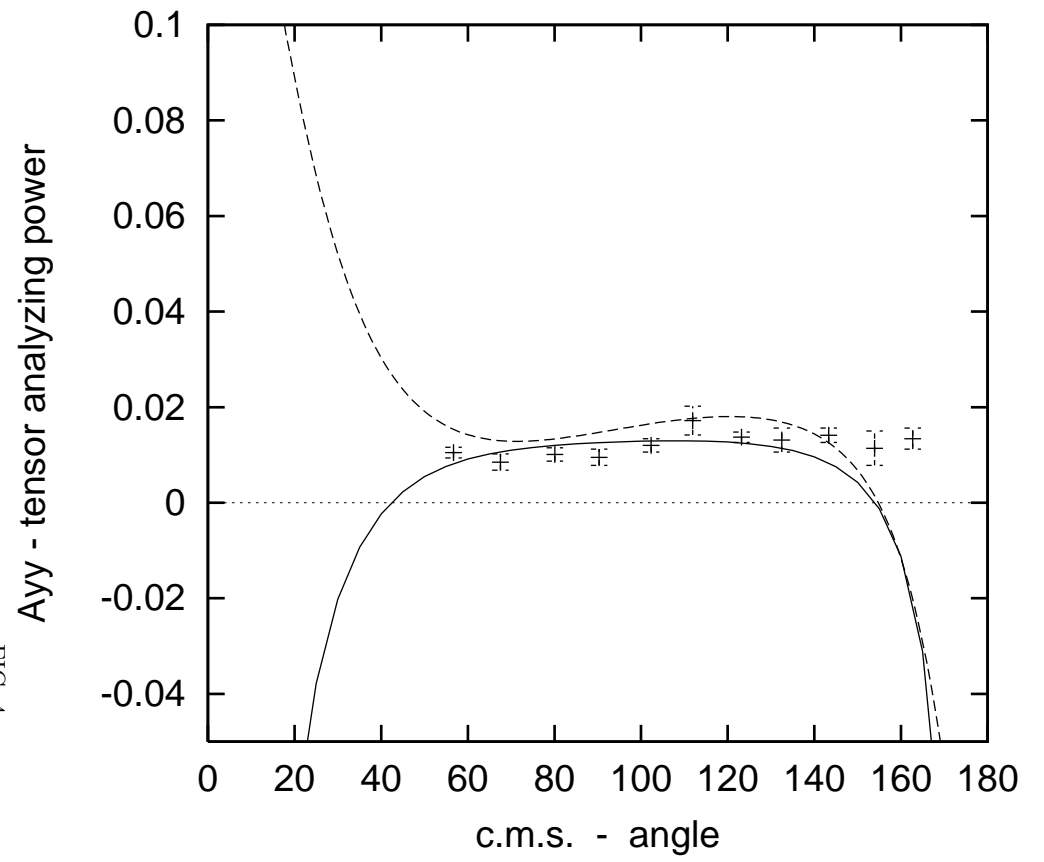


FIG. 5.

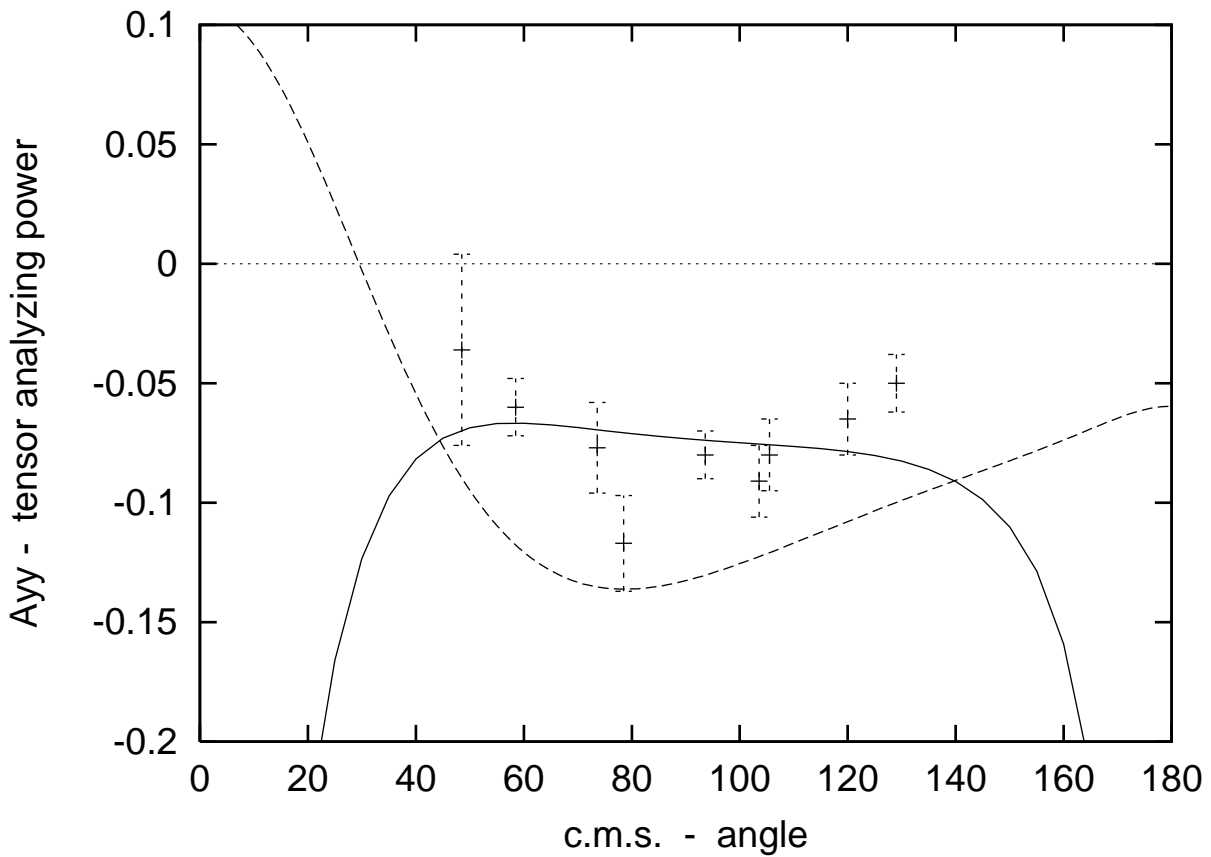


FIG. 6.

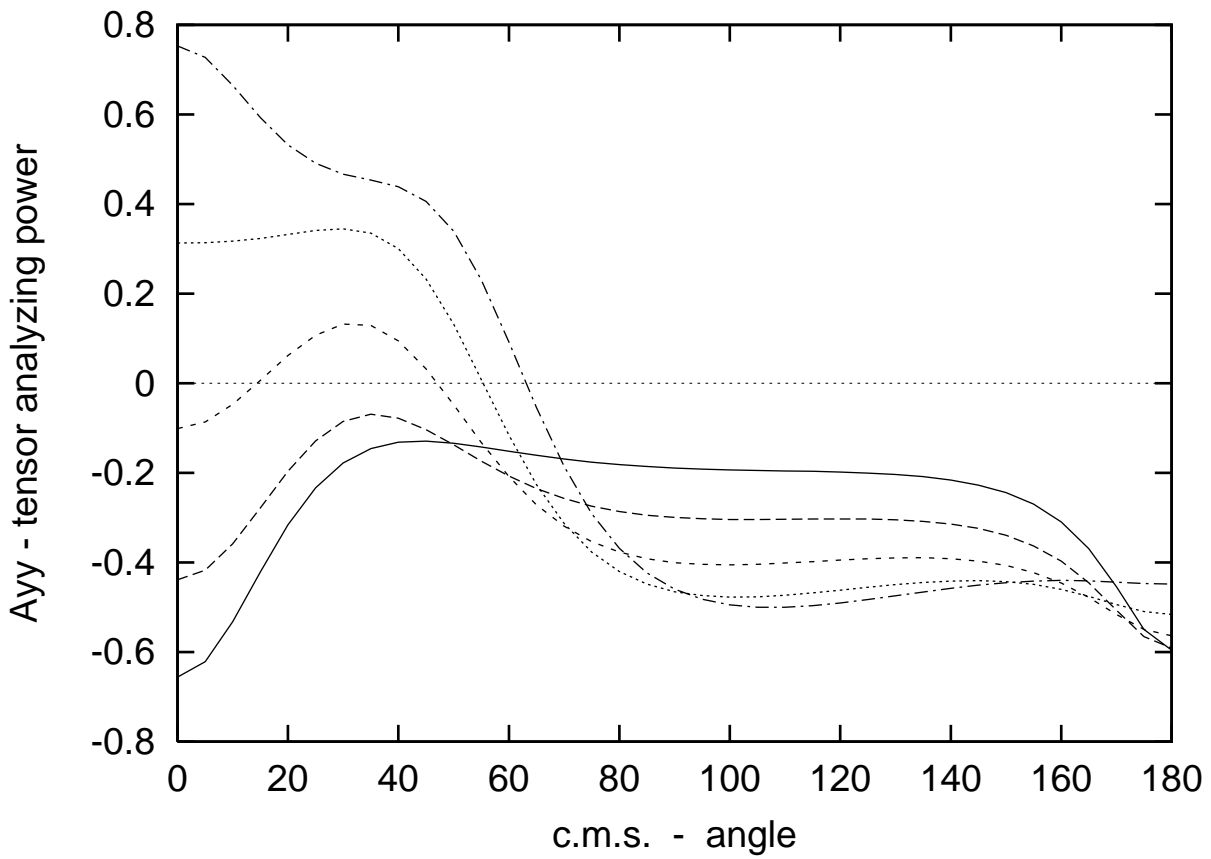


FIG. 8.

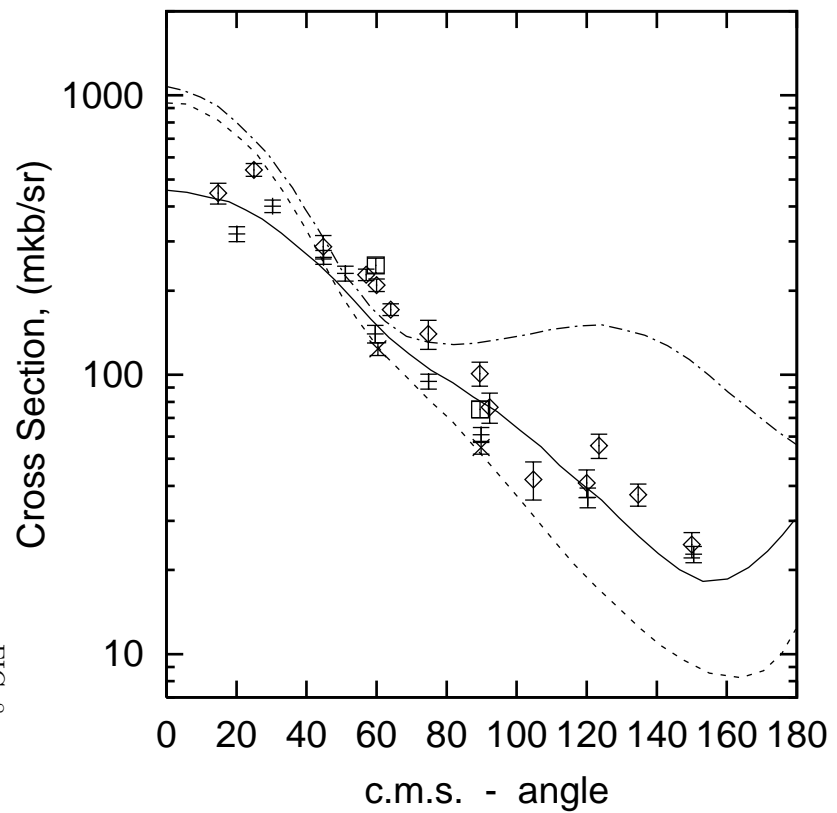


FIG. 7.

